

# Transition Metal Diazoalkane Complexes. Synthesis, Structure, and Photochemistry of $\text{Rh}[\text{C}(\text{N}_2)\text{SiMe}_3](\text{PEt}_3)_3$

Eric Deydier,<sup>†</sup> Marie-Joëlle Menu,<sup>†</sup> Michèle Dartiguenave,<sup>\*,†</sup> Yves Dartiguenave,<sup>†</sup> Michel Simard,<sup>‡</sup> André L. Beauchamp,<sup>‡</sup> John C. Brewer,<sup>§</sup> and Harry B. Gray<sup>§</sup>

Laboratoire de Chimie Inorganique, Université P. Sabatier, 118, route de Narbonne, 31062 Toulouse, France, Département de Chimie, Université de Montréal, C. P. 6128, Succ. Centre Ville, Montréal, Québec H3C 3J7, Canada, and Division of Chemistry and Chemical Engineering, California Institute of Technology, Pasadena, California 91125

Received June 26, 1995<sup>⊗</sup>

Reaction of  $\text{RhCl}(\text{PR}_3)_n$  ( $\text{R} = \text{Me}$  ( $n = 4$ ),  $\text{Et}$  ( $n = 3$ )) and  $\text{RhCl}(\text{CO})(\text{PEt}_3)_2$  with (trimethylsilyl)diazomethyl lithium at  $-78^\circ\text{C}$  in ether yields the three complexes  $\text{Rh}[\text{C}(\text{N}_2)\text{SiMe}_3](\text{PEt}_3)_3$  (**1**),  $\text{Rh}[\text{C}(\text{N}_2)\text{SiMe}_3](\text{PMe}_3)_4$  (**2**), and  $\text{Rh}[\text{C}(\text{N}_2)\text{SiMe}_3](\text{CO})(\text{PEt}_3)_2$  (**3**). **2** could not be isolated as a solid at room temperature but **1** was precipitated as red crystals that were stable enough to be handled under argon. X-ray work on **1** reveals a tetrahedrally distorted square-planar geometry with the planar (trimethylsilyl)diazomethyl ligand roughly perpendicular to the  $\text{P}_3\text{RhC}$  coordination plane. This distortion makes the  $\text{PEt}_3$  ligands nonequivalent in the crystal and produces an ABB'X pattern in the solid-state  $^{31}\text{P}$  NMR spectrum. Photolysis of  $\text{Rh}[\text{C}(\text{N}_2)\text{SiMe}_3](\text{PEt}_3)_3$  leads quantitatively to the dimer  $[\text{Rh}\{\text{C}(\text{SiMe}_3)(\text{PEt}_3)\}(\text{PEt}_3)_2]_2$  (**4**). The presence of the two ylide bridges and terminal phosphines is deduced from the COSY  $^{31}\text{P}$ – $^{31}\text{P}$  NMR spectrum. This photochemical reactivity suggests that the transient carbene  $(\text{PEt}_3)_3\text{Rh}\ddot{\text{C}}(\text{SiMe}_3)$  is electrophilic, which is typical of a singlet carbene. We believe the singlet state is stabilized by the presence of the electron-rich low-spin  $\text{Rh}(\text{PEt}_3)_3$  fragment. Reaction with  $^n\text{BuNC}$  and  $^t\text{BuNC}$  leads to stereo- and regioselective formation of a triazole that is  $\sigma$  bonded to the rhodium center. The X-ray structure of the  $^t\text{BuNC}$  derivative  $\text{Rh}[\overline{\text{CC}(\text{SiMe}_3)\text{N}_2\text{N}^t\text{Bu}}](^t\text{BuNC})_2(\text{PEt}_3)$  (**5**) shows a distorted square-planar geometry around Rh with the planar triazolato ligand roughly orthogonal to this plane. The probable reaction mechanism involves addition and substitution reactions of isocyanides at Rh followed by insertion into the Rh–C bond.

## Introduction

Diazoalkanes  $\text{R}^1\text{R}^2\text{C}(\text{N}_2)$  are versatile reagents in organic synthesis.<sup>1</sup> In inorganic and organometallic chemistry, they provide a number of interesting ligand systems, although in many cases they are catalytically decomposed by transition metals.<sup>2</sup> Complexes that result from the interaction of diazoalkanes with transition metals through the nitrogen atoms can be either nitrogen containing, in which case the diazoalkane molecule remains essentially intact, or nitrogen-free, whereby  $\text{N}_2$  loss results in carbene-related complexes. Moreover, when the diazoalkane remains unaltered, it can be N-coordinated to a single metal, with examples known for end-on and side-on coordinations, or to more than one metal in a variety of bridging modes.<sup>3</sup>

Coordination to one metal *via* the carbon atom is also observed, giving C-bonded diazoalkanes. Such  $\alpha$ -meta-

lated diazoalkanes  $\text{L}_n\text{MC}(\text{N}_2)\text{R}$  open a new area of diazoalkane chemistry, that of reactivity tuning. This can be accomplished through changes in metal electronic structure, ligand electronic and steric properties, and metal bond unsaturation. This is an important advantage since carbene reactivity is dramatically dependent on the nature of the  $\text{L}_n\text{M}$  fragment.<sup>4</sup>

Even though many N-bonded substituted transition metal diazoalkanes  $\text{L}_n\text{MN}_2\text{CR}^1\text{R}^2$  have been studied in connection with nitrogen activation, only four series of C-bonded transition metal compounds  $\text{L}_n\text{MC}(\text{N}_2)\text{R}^1$  have been isolated and described in the literature: (1) palladium complexes reported by Murahashi,<sup>5</sup> (2) osmium complexes described by Roper,<sup>6</sup> and (3) rhodium<sup>7</sup> and (4) nickel<sup>8</sup> complexes synthesized in our laboratory. A manganese diazoalkane also has been proposed as a

(3) Hillhouse, G. L.; Haymore, B. L. *J. Am. Chem. Soc.* **1982**, *104*, 1537. Bell, L. K.; Herrmann, W. A.; Kriechbaum, G. W.; Pfisterer, H.; Ziegler, M. L. *J. Organomet. Chem.* **1982**, *240*, 381. Woodcock, C.; Eisenberg, R. *Organometallics* **1985**, *4*, 4. Cowie, M.; Loeb, S. J.; McKeer, I. R. *Organometallics* **1986**, *5*, 854. Wolf, J.; Brandt, L.; Fries, A.; Werner, H. *Angew. Chem., Int. Ed. Engl.* **1990**, *29*, 510. Mizobe, Y.; Ishii, Y.; Hidai, M. *Coord. Chem. Rev.* **1995**, *139*, 281.

(4) Carter, E. A.; Goddard, W. A., III *J. Am. Chem. Soc.* **1986**, *108*, 2180, 4746.

(5) Murahashi, S. I.; Kitani, Y.; Hosokawa, T.; Miki, K.; Kasai, N. *J. Chem. Soc., Chem. Commun.* **1979**, 450.

(6) Gallo, M. A.; Jones, T. C.; Rickard, C. E. F.; Roper, W. R. *J. Chem. Soc., Chem. Commun.* **1984**, 1002.

(7) Menu, M. J.; Desrosiers, P.; Dartiguenave, M.; Dartiguenave, Y.; Bertrand, G. *Organometallics* **1987**, *6*, 1822.

(8) Menu, M. J.; König, H.; Dartiguenave, M.; Dartiguenave, Y.; Klein, H. F. *J. Am. Chem. Soc.* **1990**, *112*, 5351.

<sup>†</sup> Université P. Sabatier.

<sup>‡</sup> Université de Montréal.

<sup>§</sup> California Institute of Technology.

<sup>⊗</sup> Abstract published in *Advance ACS Abstracts*, January 1, 1996.

(1) (a) Patai, S. *The Chemistry of Diazonium and Diazo Groups*; J. Wiley and Sons: New York, 1978; Parts I and II, Chapter 18, p 859. (b) Regitz, M.; Maas, G. *Diazo Compounds: Properties and Synthesis*; Academic Press, Inc.: Orlando, FL, 1986.

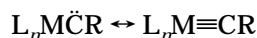
(2) Herrmann, W. A. *Angew. Chem., Int. Ed. Engl.* **1978**, *17*, 800. Brown, M. P.; Fisher, J. R.; Franklin, S. J.; Puddephatt, R. J. *J. Chem. Soc., Chem. Commun.* **1978**, 749. Clauss, A. D.; Dimas, P. A.; Sharpley, J. R. *J. Organomet. Chem.* **1980**, *201*, C31. Clauss, A. D.; Shapley, J. R.; Wilson, S. R. *J. Am. Chem. Soc.* **1981**, *103*, 7387. Dimas, P. A.; Shapley, J. R. *J. Organomet. Chem.* **1982**, *228*, C12.

reaction intermediate.<sup>9</sup> At the moment, the synthesis of such compounds is underdeveloped and their chemistry is virtually unexplored. In contrast, derivatives containing metals such as lithium, silver, mercury, or tin coordinated to carbon are well-known as diazoalkane transfer reagents.<sup>1</sup>

Our interest in C-metalated diazoalkanes arose from the reported thermally and photochemically controlled N<sub>2</sub> loss by the osmium complex OsICl[C(N<sub>2</sub>)CO<sub>2</sub>Et](NO)-(PPh<sub>3</sub>)<sub>2</sub> leading to OsICl[PPh<sub>2</sub>C<sub>6</sub>H<sub>4</sub>CHCO<sub>2</sub>Et](NO)-(PPh<sub>3</sub>) via a transient osmium-carbene species. Similarly, reacting the mercury diazo compound Hg[C(N<sub>2</sub>)CO<sub>2</sub>Et]<sub>2</sub> with MnBr(CO)<sub>5</sub> led to the isolation of an Mn dimer with a bis(alkylidyne) bridge, whose synthesis implied a manganese-carbyne moiety as an intermediate.<sup>10</sup> More recently, we found that photolysis of the (trimethylsilyl)diazomethylnickel(II) complex NiCl[C(N<sub>2</sub>)SiMe<sub>3</sub>](PMe<sub>3</sub>)<sub>2</sub> generated the Ni dimer {NiCl[C(SiMe<sub>3</sub>)(PMe<sub>3</sub>)]<sub>2</sub> via a singlet carbene intermediate.<sup>8</sup>

In the above reactions, the production of osmium- and nickel-substituted singlet carbenes as intermediates was suggested by chemical reactivities. The carbenes were trapped by insertion into the C-H bond of a PPh<sub>3</sub> phenyl ring in the former case and by nucleophilic attack of a phosphine with formation of a phosphorus ylide complex in the latter case.

In contrast, thermolysis of diazopalladium complexes leads only to decomposition.<sup>11</sup> Terminal metal-carbyne species, which correspond to one of the resonance forms of an  $\alpha$ -metalated carbene, have not been observed.



In a previous communication, we described the synthesis of the first Rh(III) diazoalkane complex, RhIME[C(N<sub>2</sub>)SiMe<sub>3</sub>](PMe<sub>3</sub>)<sub>3</sub>.<sup>7</sup> The (trimethylphosphine)rhodium(I) compound Rh[C(N<sub>2</sub>)SiMe<sub>3</sub>](PMe<sub>3</sub>)<sub>4</sub> eluded isolation as a solid at room temperature but was characterized in solution. We now report the synthesis and structural characterization of the first stable rhodium(I)-(trimethylsilyl)diazomethyl complex Rh[C(N<sub>2</sub>)SiMe<sub>3</sub>](PEt<sub>3</sub>)<sub>3</sub> (**1**) and some of its derivatives. As a carbene precursor, the complex gives rise to a reactive electrophilic carbene intermediate that is trapped by nucleophiles (e.g., PEt<sub>3</sub>). As a diazoalkane, it reacts by [3 + 2] dipolar addition with isocyanides CNR to give, with stereo- and regioselectivity, 1*H*-1,2,3-triazole C-bonded to rhodium in good yield.<sup>12</sup> Thus, the diazo complex **1** provides an easily accessible starting material to study late transition metal diazomethyl and carbene chemistry.

## Experimental Section

**Materials and Methods.** Solvent distillations and all other manipulations were performed under an argon atmosphere using standard Schlenk techniques. Tetrahydrofuran

and ether were distilled over Na/benzophenone before use. Pentane, cyclopentane, and benzene were distilled from Na just before use. All solvents were degassed by three freeze-thaw cycles. PMe<sub>3</sub>,<sup>13</sup> HC(N<sub>2</sub>)SiMe<sub>3</sub>,<sup>14</sup> [RhCl(C<sub>2</sub>H<sub>4</sub>)<sub>2</sub>]<sub>2</sub>,<sup>15</sup> RhCl-(PMe<sub>3</sub>)<sub>4</sub>,<sup>16</sup> RhCl(PEt<sub>3</sub>)<sub>3</sub>,<sup>17</sup> and RhCl(PPh<sub>3</sub>)<sub>3</sub><sup>18</sup> were synthesized by literature methods. The purity of the ligands PEt<sub>3</sub>, <sup>t</sup>BuNC, and <sup>n</sup>BuNC (Aldrich) was checked by NMR.

Infrared spectra of compounds were recorded on a Perkin-Elmer 983 spectrometer as Nujol mulls or as benzene-*d*<sub>6</sub> or pentane solutions prepared in a glovebox. The <sup>1</sup>H, <sup>31</sup>P{<sup>1</sup>H}, and <sup>13</sup>C{<sup>1</sup>H} solution spectra were recorded on a Bruker WM 200 or WH 80 spectrometer using C<sub>6</sub>D<sub>6</sub> and C<sub>7</sub>D<sub>8</sub> as solvents. Chemical shifts were referenced to the residual solvent signals for <sup>1</sup>H and <sup>13</sup>C NMR (C<sub>6</sub>D<sub>6</sub>:  $\delta_{1H} = 7.27$  and  $\delta_{13C} = 128.4$  ppm. C<sub>7</sub>D<sub>8</sub>:  $\delta_{1H} = 2.3$  and  $\delta_{13C} = 21.3$  ppm), and for <sup>31</sup>P NMR to external H<sub>3</sub>PO<sub>4</sub> (85% in D<sub>2</sub>O,  $\delta = 0$  ppm).

A high-resolution solid-state <sup>31</sup>P NMR spectrum was obtained by combining proton dipolar decoupling, magic angle spinning, and <sup>1</sup>H-<sup>31</sup>P cross polarization. The Varian 300 spectrometer operated at 299.949 MHz for <sup>1</sup>H and 121.423 MHz for <sup>31</sup>P. The acquisition parameters were as follows: cross polarization time 0.2 ms; pulse interval 80 ms; 200 accumulations; magic angle spinning rate 4.5 kHz.

For the COSY <sup>31</sup>P-<sup>31</sup>P experiment, 256 FIDs of eight scans each, consisting of 2 K data points, were accumulated. The acquisition parameters were as follows: spectral width 2690 Hz; acquisition time 0.166 s; relaxation delay 1.0 s; pulse width 90°; gated decoupling, spin rate 25 Hz. Data processing was pseudo-echo-shaped.

**Crystallographic Work.** X-ray diffraction work on both compounds was carried out with an Enraf-Nonius CAD-4 diffractometer using graphite-monochromatized Cu K $\alpha$  radiation. A reduced cell was determined from 25 reflections on a rotation photograph, and final cell parameters were calculated by least-squares refinement on 25 higher angle reflections ( $20^\circ < \theta < 25^\circ$ ) obtained from a quick precollection. Intensity data were collected using the  $\omega/2\theta$  scan technique ( $\Delta\omega = (0.80 + 0.14 \tan \theta)^\circ$ ). Four standards were used to monitor intensity every hour and orientation every 200 measurements. Crystal data for both compounds are given in Table 1.

The structures were solved by the heavy-atom method and refined on  $|F_o|$  by the full-matrix least-squares methods of the SHELX-76 package.<sup>19</sup> Individual weights  $\omega = [\sigma^2(F_o) + 0.0001(F_o)^2]^{-1}$  were applied. The non-hydrogen atoms were refined anisotropically, whereas the hydrogens were placed at idealized positions and repositioned after each cycle. The scattering factors used were from standard sources.<sup>20,21</sup> The anomalous dispersion contributions of Rh, Si, and P were taken into account.<sup>22</sup>

**Crystal Structure Analysis of 1.** The compound crystallized from pentane as red needles. A section of a needle (0.50  $\times$  0.50  $\times$  0.08 mm<sup>3</sup>) was mounted quickly on the diffractometer at -100 °C. The Niggli matrix unambiguously ruled out all Laue symmetries higher than triclinic. The structure was successfully solved and refined in the centric  $P\bar{1}$  space group. A half-sphere of data was collected. The intensities of the standard reflections decreased smoothly because of slow crystal decomposition: the data were scaled accordingly at the data reduction stage. The data were corrected for the absorption

(13) Wolfberger, W.; Schmidbaur, H. *Synth. React., Inorg. Met. Org. Chem.* **1974**, *4*, 149.

(14) Martin, M. *Synth. Commun.* **1983**, *13*, 809.

(15) Cramer, R. *Inorg. Chem.* **1962**, *1*, 722.

(16) Werner, H.; Feser, R.; Buchner, W. *Chem. Ber.* **1979**, *112*, 834.

(17) Intille, G. M. *Inorg. Chem.* **1972**, *11*, 695.

(18) Osborn, J. A.; Jardine, F. H.; Young, J. F.; Wilkinson, G. J. *Chem. Soc. A* **1966**, 1711.

(19) Sheldrick, G. M. SHELX76, *Program for crystal structure determinations*; University of Cambridge, Cambridge, England, 1976.

(20) Cromer, D. T.; Mann, J. B. *Acta Crystallogr.* **1968**, *A24*, 321.

(21) Stewart, R. F.; Davidson, E. R.; Simpson, W. T. *J. Chem. Phys.* **1965**, *42*, 3175.

(22) Cromer, D. T.; Liberman, D. *J. Chem. Phys.* **1970**, *53*, 1891.

(9) Herrmann, W. A. *Angew. Chem., Int. Ed. Engl.* **1974**, *13*, 599. Kandler, H.; Bosch, H. W.; Shklover, V.; Berke, H. *J. Organomet. Chem.* **1991**, *409*, 233.

(10) Herrmann, W. A. *Angew. Chem., Int. Ed. Engl.* **1974**, *13*, 812. Herrmann, W. A.; Reiter, B.; Biersack, H. *J. Organomet. Chem.* **1975**, *97*, 245. Redhouse, A. D. *J. Organomet. Chem.* **1975**, *99*, C25.

(11) Murahashi, S. I.; Kitani, Y.; Uno, T.; Hosokawa, T.; Miki, K.; Yinezawa, T.; Kasai, N. *Organometallics* **1986**, *5*, 356.

(12) Deydier, E.; Menu, M. J.; Dartiguenave, M.; Dartiguenave, Y. *J. Chem. Soc., Chem. Commun.* **1991**, 809.

**Table 1. Crystallographic Data for Rh[C(N<sub>2</sub>)SiMe<sub>3</sub>](PEt<sub>3</sub>)<sub>3</sub> (1) and**

|   | Rh[CC(SiMe <sub>3</sub> )N <sub>2</sub> N( <sup>t</sup> Bu)]( <sup>t</sup> BuNC) <sub>2</sub> (PEt <sub>3</sub> ) (5) |  |
|---|---|--|
| formula   | C <sub>22</sub> H <sub>54</sub> N <sub>2</sub> P <sub>3</sub> SiRh  | C <sub>25</sub> H <sub>51</sub> N <sub>5</sub> PSiRh |
| mol wt  | 570.60  | 583.68   |
| <i>T</i> , °C                                       | −100  | −60  |
| cryst syst  | triclinic   | monoclinic   |
| space group   | <i>P</i> $\bar{1}$  | <i>P</i> 2 <sub>1</sub> / <i>c</i>                   |
| <i>a</i> , Å  | 9.753(4)  | 11.749(4)  |
| <i>b</i> , Å  | 10.082(4)   | 9.960(4)   |
| <i>c</i> , Å  | 16.199(6)   | 28.25(2)   |
| $\alpha$ , deg                                      | 84.32(3)  | 90   |
| $\beta$ , deg                                       | 80.04(3)  | 96.26(4)   |
| $\gamma$ , deg                                      | 73.28(3)  | 90   |
| <i>V</i> , Å <sup>3</sup>                           | 1501(2)   | 3286(3)  |
| <i>Z</i>  | 2   | 4  |
| <i>d</i> <sub>calc</sub> , g cm <sup>−3</sup>       | 1.263   | 1.180  |
| radiation   | Cu K $\alpha$   | Cu K $\alpha$  |
| wavelength $\lambda$ (Å)                            | 1.541 78  | 1.541 78   |
| $\mu$ (I), cm <sup>−1</sup>                         | 67.1  | 52.5   |
| 2 $\theta$ <sub>max</sub> , deg                     | 140   | 140  |
| no. of unique data                                  | 5917  | 6223   |
| no. of data with <i>I</i> > 3 $\sigma$ ( <i>I</i> ) | 4795  | 4352   |
| <i>R</i> <sup>a</sup>                               | 0.060   | 0.069  |
| <i>R</i> <sub>w</sub> <sup>a</sup>                  | 0.081   | 0.084  |
| GOF <sup>a</sup>                                    | 1.97  | 2.45   |

<sup>a</sup>  $R = \sum ||F_o| - |F_c|| / \sum |F_o|$ ;  $R_w = [\sum w(|F_o| - |F_c|)^2 / \sum w|F_o|^2]^{1/2}$ ; GOF =  $[\sum w(|F_o| - |F_c|)^2 / (\text{no. of reflns} - \text{no. of params})]^{1/2}$ .

(semiempirical program PSI of SPD;<sup>23</sup> transmission 0.52–0.99), Lorentz, and polarization effects.

The Rh atom was located from a Patterson map, and the remaining non-hydrogen atoms were found from  $\Delta F$  maps. All non-hydrogen atoms were refined anisotropically. Hydrogen positions were calculated (C–H = 0.95 Å, *B*<sub>iso</sub> = 8.0 (methyl) or 4.0 Å<sup>2</sup> (methylene)). There was no evidence of disorder in this structure. The final  $\Delta F$  map showed a general background below  $\pm 0.30$  e/Å<sup>3</sup> and six peaks in the range of  $\pm |0.4–0.9|$  e/Å<sup>3</sup> within 1.5 Å from Rh. The refined coordinates are listed in Table 2.

**Crystal Structure Analysis of 5.** A yellow crystal of dimensions 0.06 × 0.56 × 0.42 mm<sup>3</sup> was mounted in a Lindemann capillary filled with argon. Intensity data were collected as above at −60 °C. Space group *P*2<sub>1</sub>/*c* was unambiguously determined from the 2/*m* Laue symmetry, and systematic absences (*h*0*l*, *l* ≠ 2*n*; 0*k*0, *k* ≠ 2*n*) were identified in the full data set. A whole sphere of intensities (20 498 reflections) was measured. The standard reflection showed random fluctuations within  $\pm 5.7\%$  during data collection. An absorption correction based on the geometry of the crystal was applied (Gaussian integration, grid 20 × 20 × 20; transmission 0.15–0.73). Averaging yielded a set of 6223 independent reflections (*R*<sub>av</sub> = 0.049). The usual Lp correction was finally applied.

The Rh atom was located from the Patterson synthesis. The atoms directly bonded to the metal and those of the triazole unit were found from the first  $\Delta F$  map. The positions corresponded to those found from an earlier data set collected at room temperature.<sup>12</sup> The presence of multiple peaks in the next  $\Delta F$  map indicated disorder in the isocyanide and phosphine substituents. Twofold disorder about the Rh–P bond resulted in four of the phosphine carbon atoms (C20–C26) being distributed over two resolved positions. The *tert*-butyl groups in the isocyanide ligands were found to be disordered over two (C33–C36) or three (C43–C46) positions. The nondisordered atoms were refined isotropically, and the following strategy was applied for each of the disordered units. The atomic positions and a common *U*<sub>iso</sub> temperature factor were refined, assuming occupancies of 0.50 (or 0.33) for the two (or three) disordered individuals. Occupancies were then

**Table 2. Atomic Coordinates of the Non-Hydrogen Atoms of Rh[C(N<sub>2</sub>)SiMe<sub>3</sub>](PEt<sub>3</sub>)<sub>3</sub> (1)**

| atom | <i>x</i>   | <i>y</i>   | <i>z</i>   |
|------|------------|------------|------------|
| Rh   | 0.08246(4) | 0.19309(4) | 0.23966(2) |
| P1   | −0.0724(1) | 0.0669(1)  | 0.2205(1)  |
| P2   | 0.1888(1)  | 0.3724(1)  | 0.2011(1)  |
| P3   | 0.2919(1)  | 0.0234(1)  | 0.2427(1)  |
| Si   | −0.2102(2) | 0.3738(2)  | 0.3876(1)  |
| N1   | −0.1783(5) | 0.4461(5)  | 0.2297(3)  |
| N2   | −0.2361(6) | 0.5336(6)  | 0.1845(4)  |
| C1   | −0.1147(5) | 0.3508(5)  | 0.2792(4)  |
| C2   | −0.1138(8) | 0.2426(7)  | 0.4628(4)  |
| C3   | −0.2297(3) | 0.5526(7)  | 0.4196(5)  |
| C4   | −0.4004(7) | 0.3603(7)  | 0.3955(5)  |
| C11  | −0.0032(7) | −0.0864(6) | 0.1568(4)  |
| C12  | −0.1115(9) | −0.1535(7) | 0.1331(6)  |
| C13  | −0.1888(6) | 0.0050(6)  | 0.3096(4)  |
| C14  | −0.1062(8) | −0.1075(7) | 0.3665(5)  |
| C15  | −0.2170(6) | 0.1716(6)  | 0.1619(4)  |
| C16  | −0.1609(9) | 0.2272(8)  | 0.0751(5)  |
| C21  | 0.3854(6)  | 0.3610(6)  | 0.1812(4)  |
| C22  | 0.4304(7)  | 0.4855(7)  | 0.1335(5)  |
| C23  | 0.1225(7)  | 0.5255(6)  | 0.2646(4)  |
| C24  | 0.1628(8)  | 0.4935(7)  | 0.3526(5)  |
| C25  | 0.1356(6)  | 0.4422(6)  | 0.0985(4)  |
| C26  | 0.2089(8)  | 0.3442(8)  | 0.0276(4)  |
| C31  | 0.2806(6)  | −0.1493(6) | 0.2878(5)  |
| C32  | 0.4162(8)  | −0.2543(7) | 0.3112(6)  |
| C33  | 0.4293(7)  | −0.0239(6) | 0.1481(5)  |
| C34  | 0.3791(9)  | −0.0822(8) | 0.0800(5)  |
| C35  | 0.4043(6)  | 0.0597(6)  | 0.3139(5)  |
| C36  | 0.3278(9)  | 0.0845(9)  | 0.4043(6)  |

allowed to refine as well. At this stage, occupancies were adjusted so that all atoms in a given individual have the same value and the sum of the occupancies for the two (or three) individuals be equal to unity. These occupancy factors were fixed for the rest of the refinement. Whole and fractional hydrogens were also fixed at idealized positions (C–H = 0.95 Å), but a common *U*<sub>iso</sub> temperature factor was refined for the three or two hydrogens of each given methyl (or methylene) group. All non-hydrogen atomic sites were refined anisotropically. The final  $\Delta F$  map showed a general background below  $\pm 0.49$  e/Å<sup>3</sup> and six peaks in the range of  $\pm |0.5–0.6|$  e/Å<sup>3</sup> within 1.5 Å from Rh. The refined coordinates are listed in Table 3.

**Synthesis. Rh[C(N<sub>2</sub>)SiMe<sub>3</sub>](PEt<sub>3</sub>)<sub>3</sub> (1).** PEt<sub>3</sub> (1.5 mL) was slowly added to 500 mg (1.28 mmol) of the Cramer complex [RhCl(C<sub>2</sub>H<sub>4</sub>)<sub>2</sub>]<sub>2</sub> dissolved in 20 mL of ether. The color of the solution turned red immediately, implying rapid formation of RhCl(PEt<sub>3</sub>)<sub>3</sub>. After stirring this solution for 15 min, the solvent was evaporated. LiCN<sub>2</sub>SiMe<sub>3</sub> (2.8 mmol, 0.32 g of HCN<sub>2</sub>SiMe<sub>3</sub> in 15 mL of ether + 1.76 mL of MeLi (1.6 M in hexane) at −78 °C, 25 min stirring) was transferred at low temperature onto this crude product. After 1 h, the temperature was slowly increased to room temperature. Evaporation of the solvent *in vacuo* and recrystallization from 20 mL of pentane gave 122 mg of red crystals of **1**. Yield: 84%. Anal. Calcd for C<sub>22</sub>H<sub>54</sub>P<sub>3</sub>N<sub>2</sub>SiRh: C, 46.31; H, 9.54; N, 4.91. Found: C, 45.82; H, 9.22; N, 4.62. IR (cm<sup>−1</sup>) pentane: 1945 (C(N<sub>2</sub>)). <sup>1</sup>H NMR (C<sub>6</sub>D<sub>6</sub>, 293 K): 0.6 (9H, s, SiMe<sub>3</sub>); 1.04 (9H, dt, <sup>3</sup>*J*<sub>PH</sub> = 14 Hz, <sup>3</sup>*J*<sub>HH</sub> = 7.5 Hz, CH<sub>3</sub>CH<sub>2</sub>P); 1.16 (18H, dt, <sup>3</sup>*J*<sub>PH</sub> = 14 Hz, <sup>3</sup>*J*<sub>HH</sub> = 7.5 Hz, CH<sub>3</sub>CH<sub>2</sub>P); 1.43 (6H, dq, <sup>2</sup>*J*<sub>PH</sub> = 7 Hz, <sup>3</sup>*J*<sub>HH</sub> = 7.5 Hz, CH<sub>3</sub>CH<sub>2</sub>P); 1.83 (12H, br, CH<sub>3</sub>CH<sub>2</sub>P). <sup>13</sup>C NMR (C<sub>6</sub>D<sub>6</sub>, 293 K): 1.5 (s, SiMe<sub>3</sub>); 9.5 (s, CH<sub>3</sub>CH<sub>2</sub>P<sub>1,2</sub>); 9.6 (s, CH<sub>3</sub>CH<sub>2</sub>P<sub>3</sub>); 19.0 (t, CH<sub>3</sub>CH<sub>2</sub>P<sub>1,2</sub>, *J*<sub>CP</sub> = 11 Hz); 26 (d, CH<sub>3</sub>CH<sub>2</sub>P<sub>3</sub>, *J*<sub>PC</sub> = 20 Hz).

**Rh[C(N<sub>2</sub>)SiMe<sub>3</sub>](PMe<sub>3</sub>)<sub>4</sub> (2).** RhCl(PMe<sub>3</sub>)<sub>4</sub> (1.78 g, 4 mmol) and Li(CN<sub>2</sub>)SiMe<sub>3</sub> (0.57 g (5 mmol), HC(N<sub>2</sub>)SiMe<sub>3</sub> + 2.8 mL (5 mmol) of MeLi, stirred at −78 °C in 15 mL of Et<sub>2</sub>O for 25 min) were reacted in a procedure analogous to that given for **1**. Identical workup gave an orange pentane solution. Unfortunately, attempts to isolate this complex as a solid at room temperature led only to decomposition. IR (cm<sup>−1</sup>) pentane: 1950 (ν(CN<sub>2</sub>)). <sup>1</sup>H NMR (C<sub>6</sub>D<sub>6</sub>, 293 K): 0.37 (9H, s, SiMe<sub>3</sub>); 1.22 (36H, br, CH<sub>3</sub>).

(23) Frenz, B. A. *Enraf-Nonius Structure Determination Package*, 1985.

**Table 3. Atomic Coordinates of the Non-Hydrogen Atoms of Rh[CC(SiMe<sub>3</sub>)N<sub>2</sub>N(<sup>t</sup>Bu)](<sup>t</sup>BuNC)<sub>2</sub>(PEt<sub>3</sub>)<sub>2</sub> (5)**

| atom <sup>a</sup> | x           | y           | z           |
|-------------------|-------------|-------------|-------------|
| Rh                | 0.27540(5)  | 0.67645(6)  | 0.12593(2)  |
| P                 | 0.44323(16) | 0.56415(22) | 0.12651(8)  |
| Si                | 0.2097(2)   | 1.0446(2)   | 0.15896(9)  |
| N3                | -0.0055(6)  | 0.9546(7)   | 0.1242(2)   |
| N4                | -0.0632(5)  | 0.8497(8)   | 0.1081(2)   |
| N5                | 0.0126(5)   | 0.7456(7)   | 0.1066(2)   |
| N32               | 0.2301(6)   | 0.5907(8)   | 0.2275(3)   |
| N42               | 0.2759(6)   | 0.7987(6)   | 0.0250(2)   |
| C1                | 0.1232(6)   | 0.7846(7)   | 0.1219(2)   |
| C2                | 0.1094(6)   | 0.9227(8)   | 0.1339(2)   |
| C6                | -0.0355(4)  | 0.6104(5)   | 0.0926(2)   |
| C7                | -0.1446(8)  | 0.6275(9)   | 0.0563(4)   |
| C8                | -0.0671(8)  | 0.5373(9)   | 0.1380(3)   |
| C9                | 0.0530(7)   | 0.5250(8)   | 0.1067(3)   |
| C10               | 0.3496(7)   | 1.0238(9)   | 0.1403(4)   |
| C11               | 0.1554(9)   | 1.2099(8)   | 0.1412(4)   |
| C12               | 0.2236(10)  | 1.0307(11)  | 0.2234(3)   |
| C21 <sup>a</sup>  | 0.4652(17)  | 0.4247(20)  | 0.1668(8)   |
| C22 <sup>a</sup>  | 0.5762(15)  | 0.3495(17)  | 0.1700(7)   |
| C23 <sup>a</sup>  | 0.4665(11)  | 0.4845(14)  | 0.0702(5)   |
| C24               | 0.3784(11)  | 0.3830(13)  | 0.0520(4)   |
| C25 <sup>a</sup>  | 0.5749(13)  | 0.6743(17)  | 0.1398(8)   |
| C26               | 0.5854(11)  | 0.7736(14)  | 0.1017(7)   |
| C21 <sup>b</sup>  | 0.5100(21)  | 0.4863(29)  | 0.1831(11)  |
| C22 <sup>b</sup>  | 0.4670(32)  | 0.3959(38)  | 0.2080(12)  |
| C23 <sup>b</sup>  | 0.4289(32)  | 0.3858(37)  | 0.0944(13)  |
| C25 <sup>b</sup>  | 0.5567(31)  | 0.6268(31)  | 0.0971(17)  |
| C31               | 0.2490(6)   | 0.6199(8)   | 0.1900(3)   |
| C33 <sup>a</sup>  | 0.1817(20)  | 0.5358(17)  | 0.2731(8)   |
| C34               | 0.1222(11)  | 0.6632(10)  | 0.2894(4)   |
| C35 <sup>a</sup>  | 0.0922(22)  | 0.4257(26)  | 0.2614(9)   |
| C36 <sup>a</sup>  | 0.2751(18)  | 0.4906(25)  | 0.3054(8)   |
| C33 <sup>b</sup>  | 0.2045(28)  | 0.5800(27)  | 0.2726(13)  |
| C35 <sup>b</sup>  | 0.1587(28)  | 0.4288(36)  | 0.2694(11)  |
| C36 <sup>b</sup>  | 0.3161(25)  | 0.5715(34)  | 0.3094(10)  |
| C41               | 0.2827(6)   | 0.7493(8)   | 0.0619(3)   |
| C43 <sup>c</sup>  | 0.2380(21)  | 0.8645(14)  | -0.0173(8)  |
| C44 <sup>d</sup>  | 0.2383(19)  | 1.0197(14)  | -0.0044(6)  |
| C45 <sup>d</sup>  | 0.1230(26)  | 0.8299(34)  | -0.0331(14) |
| C46 <sup>d</sup>  | 0.3231(42)  | 0.8430(37)  | -0.0548(11) |
| C44 <sup>e</sup>  | 0.1785(39)  | 0.7994(45)  | -0.0533(18) |
| C45 <sup>e</sup>  | 0.3478(49)  | 0.9062(64)  | -0.0380(19) |
| C46 <sup>e</sup>  | 0.1392(42)  | 0.9674(50)  | -0.0013(15) |
| C43 <sup>e</sup>  | 0.2270(47)  | 0.9037(32)  | -0.0134(16) |
| C44 <sup>e</sup>  | 0.3110(52)  | 0.9884(50)  | -0.0233(20) |
| C45 <sup>e</sup>  | 0.0808(29)  | 0.8706(65)  | -0.0137(19) |
| C46 <sup>e</sup>  | 0.2358(49)  | 0.7992(53)  | -0.0590(17) |

<sup>a</sup> Occupancy factors: a = 0.55; b = 0.45; c = 0.70; e = 0.30.

**Rh[C(N<sub>2</sub>)SiMe<sub>3</sub>](CO)(PEt<sub>3</sub>)<sub>2</sub> (3). Method A.** A solution of LiC(N<sub>2</sub>)SiMe<sub>3</sub> (-78 °C, 1.3 mL (2.1 mmol) of MeLi + 290 mg (2.5 mmol) of H(CN<sub>2</sub>)SiMe<sub>3</sub> in 15 mL of Et<sub>2</sub>O, 25 min stirring) was added dropwise to 800 mg (2.0 mmol) of RhCl(CO)(PEt<sub>3</sub>)<sub>2</sub>, which previously had been prepared by addition of HCHO onto RhCl(PEt<sub>3</sub>)<sub>3</sub>. The mixture was kept at -78 °C for 20 min and then at room temperature for 30 min. Removal of Et<sub>2</sub>O *in vacuo* gave a yellow residue. This was dissolved in 15 mL of cold pentane. After filtration, the solution was concentrated and cooled to -40 °C to afford an oily residue. Workup and recrystallization from pentane gave 380 mg of a light yellow solid, **3**. Yield: 40%. Anal. Calcd for C<sub>17</sub>H<sub>39</sub>N<sub>2</sub>O<sub>2</sub>RhSi: C, 42.5; H, 8.18; N, 5.83. Found: C, 41.4; H, 8.12; N, 5.52. IR (cm<sup>-1</sup>) Nujol: 1961, s, (C(N<sub>2</sub>)); 1947 vs. (CO). <sup>1</sup>H NMR (C<sub>6</sub>D<sub>6</sub>, 293 K): 0.4 (9H, s, SiMe<sub>3</sub>); 1.11 (18H, dt, <sup>3</sup>J<sub>PH</sub> = 15.5 Hz, <sup>3</sup>J<sub>HH</sub> = 7.5 Hz, CH<sub>3</sub>CH<sub>2</sub>P); 1.83 (12H, br, CH<sub>3</sub>CH<sub>2</sub>P). <sup>13</sup>C NMR (C<sub>7</sub>D<sub>8</sub>, 203 K): 1.0 (s, SiMe<sub>3</sub>); 8.8 (s, CH<sub>3</sub>CH<sub>2</sub>P); 11.2 (dt, <sup>2</sup>J<sub>CP</sub> = 14 Hz, <sup>1</sup>J<sub>CRh</sub> = 28 Hz, C(N<sub>2</sub>)); 17.2 (s, CH<sub>3</sub>CH<sub>2</sub>P); 191.8 (dt, <sup>1</sup>J<sub>CP</sub> = 15 Hz, <sup>1</sup>J<sub>CRh</sub> = 64 Hz, CO).

**Method B.** CO was quantitatively bubbled through a benzene solution (5 mL) of Rh[C(N<sub>2</sub>)SiMe<sub>3</sub>](PEt<sub>3</sub>)<sub>3</sub> (300 mg, 0.53 mmol). The solution turned yellow immediately.

Monitoring the reaction by <sup>31</sup>P NMR and elimination of benzene gave **3** as a yellow powder in 90% yield after workup.

**{Rh[C(SiMe<sub>3</sub>)(PEt<sub>3</sub>)](PEt<sub>3</sub>)<sub>2</sub>}<sub>2</sub> (4).** Rh[C(N<sub>2</sub>)SiMe<sub>3</sub>](PEt<sub>3</sub>)<sub>3</sub> (150 mg) was dissolved in 2 mL of benzene and poured into a 10 mm NMR tube. This was irradiated at 330 nm (room temperature) for 90 min in a Rayonet reactor. After this period, the solution turned green. Concentration *in vacuo* gave a green, air-sensitive oily material, which was stable up to -20 °C. Workup of the compound at room temperature gave rise to decomposition. <sup>1</sup>H NMR (C<sub>6</sub>D<sub>6</sub>, 293 K): 0.66 (9H, s, SiMe<sub>3</sub>); 1.03 (9H, dt, <sup>3</sup>J<sub>PH</sub> = 15.4 Hz, <sup>3</sup>J<sub>HH</sub> = 7.4 Hz, CH<sub>3</sub>CH<sub>2</sub>P); 1.15 (18H, dt, <sup>3</sup>J<sub>PH</sub> = 14.2 Hz, <sup>3</sup>J<sub>HH</sub> = 7.5 Hz, CH<sub>3</sub>CH<sub>2</sub>P); 1.38 (12H, m, CH<sub>3</sub>CH<sub>2</sub>P); 1.67 (6H, dq, <sup>2</sup>J<sub>PH</sub> = 11 Hz, <sup>3</sup>J<sub>HH</sub> = 7.5 Hz, CH<sub>3</sub>CH<sub>2</sub>P).

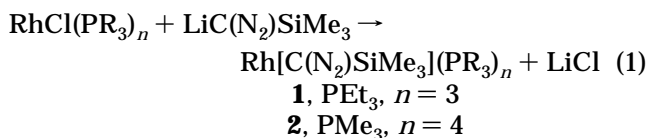
**Rh[CC(SiMe<sub>3</sub>)N<sub>2</sub>N(<sup>t</sup>Bu)](PEt<sub>3</sub>)(<sup>t</sup>BuNC)<sub>2</sub> (5).** <sup>t</sup>BuNC (175 mg, 2 mmol) was added to a solution of 300 mg (0.53 mmol) of Rh[C(N<sub>2</sub>)SiMe<sub>3</sub>](PEt<sub>3</sub>)<sub>3</sub> in 5 mL of benzene. The solution was stirred for 5 min. Filtration on Celite and removal of benzene *in vacuo* gave a yellow-brown residue that was extracted with 10 mL of pentane. The solution was concentrated to 2 mL and cooled to -50 °C to afford a yellow solid. Recrystallization from cyclopentane at -20 °C gave 200 mg of **5** as light yellow crystals. Yield: 65%. Anal. Calcd for C<sub>25</sub>H<sub>51</sub>N<sub>5</sub>PSiRh: C, 51.45; H, 8.81; N, 12. Found: C, 51.12; H, 8.57; N, 11.8. IR (cm<sup>-1</sup>) Nujol: 2100 (CN<sup>t</sup>Bu). <sup>1</sup>H NMR (C<sub>6</sub>D<sub>6</sub>, 293 K): (terminal t), in the ring (r): 0.96 (18H, CNC(CH<sub>3</sub>)<sub>3</sub>); 1.00 (9H, s, SiMe<sub>3</sub>); 1.22 (9H, dt, <sup>3</sup>J<sub>PH</sub> = 14 Hz; <sup>3</sup>J<sub>HH</sub> = 7.5 Hz; CH<sub>3</sub>CH<sub>2</sub>P); 1.57 (6H, dq, <sup>3</sup>J<sub>PH</sub> = 7 Hz; <sup>3</sup>J<sub>HH</sub> = 7.5 Hz, CH<sub>3</sub>CH<sub>2</sub>P); 2.28 (9H, s, CNC(CH<sub>3</sub>)<sub>3</sub>). <sup>13</sup>C NMR (C<sub>6</sub>D<sub>6</sub>, 293 K): 2.1 (s, SiMe<sub>3</sub>); 9.0 (s, CH<sub>3</sub>CH<sub>2</sub>P); 21.1 (d, CH<sub>3</sub>CH<sub>2</sub>P, <sup>1</sup>J<sub>CP</sub> = 22 Hz); 30.1<sup>t</sup>, 32.9<sup>r</sup>, CNC(CH<sub>3</sub>)<sub>3</sub>; 55.6<sup>t</sup>, 57.3<sup>r</sup>, CNC(CH<sub>3</sub>)<sub>3</sub>.

**Rh[CC(SiMe<sub>3</sub>)N<sub>2</sub>N(<sup>n</sup>Bu)](PEt<sub>3</sub>)<sub>2</sub>(<sup>n</sup>BuNC) (6).** This compound was prepared under conditions identical with that for

Rh[CC(SiMe<sub>3</sub>)N<sub>2</sub>N(<sup>t</sup>Bu)](PEt<sub>3</sub>)(<sup>t</sup>BuNC)<sub>2</sub>, except that the crystallization was carried out after workup in pentane. **6** (150 mg) was obtained as a light yellow solid. Yield: 46%. Anal. Calcd for C<sub>26</sub>H<sub>57</sub>N<sub>4</sub>P<sub>2</sub>SiRh: C, 50.47; H, 2.29; N, 9.06. Found: C, 49.82; H, 2.42; N, 8.92. IR (cm<sup>-1</sup>) Nujol: 2113 (CN<sup>n</sup>Bu). <sup>1</sup>H NMR (C<sub>6</sub>D<sub>6</sub>, 293 K): 0.88 (9H, s, SiMe<sub>3</sub>); 1.08 (18H, dt; <sup>3</sup>J<sub>PH</sub> = 14.5 Hz, <sup>3</sup>J<sub>HH</sub> = 7.5 Hz; CH<sub>3</sub>CH<sub>2</sub>P); 1.48 (12H, br, CH<sub>3</sub>CH<sub>2</sub>P). <sup>13</sup>C NMR (C<sub>6</sub>D<sub>6</sub>, 293 K): 2.4 (s, SiMe<sub>3</sub>); 9.1 (s, CH<sub>3</sub>CH<sub>2</sub>P); 13.6<sup>t</sup>, 14.6<sup>r</sup>, (CN(CH<sub>2</sub>)<sub>3</sub>CH<sub>3</sub>); 19.3 (t, CH<sub>3</sub>CH<sub>2</sub>P, <sup>1</sup>J<sub>CP</sub> = 12 Hz); 20.3<sup>t</sup>, 21.8<sup>r</sup>, 32.0<sup>t</sup>, 33.9<sup>r</sup>, 43.3<sup>t</sup>, 53.5<sup>r</sup>, (CN(CH<sub>2</sub>)<sub>3</sub>CH<sub>3</sub>).

## Results

**Preparation of Rh[C(N<sub>2</sub>)SiMe<sub>3</sub>](PR<sub>3</sub>)<sub>n</sub>: **1**, PEt<sub>3</sub>, *n* = **3**; **2**, PMe<sub>3</sub>, *n* = **4**.** The syntheses of the (trimethylsilyl)diazomethyl complexes Rh[C(N<sub>2</sub>)SiMe<sub>3</sub>](PR<sub>3</sub>)<sub>n</sub> by reaction of RhCl(PR<sub>3</sub>)<sub>n</sub> with LiC(N<sub>2</sub>)SiMe<sub>3</sub> in THF or ether were remarkably dependent on the identity of the phosphine. The alkylating agent LiC(N<sub>2</sub>)SiMe<sub>3</sub> was reacted with RhCl(PR<sub>3</sub>)<sub>n</sub> as shown in eq 1. The reaction



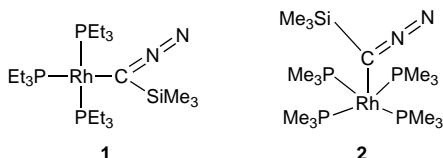
with the tris(triphenylphosphine) complex was unsuccessful. Although a color change of the solution from red to brown was observed, the starting RhCl(PPh<sub>3</sub>)<sub>3</sub> was recovered unchanged from the mixture. **1** was obtained as red crystals in 84% yield but **2** could not be obtained as a solid at room temperature in analytically pure form. Decomposition was immediate in the solid state, but started only after a few days in solution. The

**Table 4.**  $^{31}\text{P}\{^1\text{H}\}$  NMR Data<sup>a</sup>

| complex               | spin system       | $\delta\text{P}_A$ | $J_{AX}$ | $\delta\text{P}_B$ | $J_{BX}$ | $J_{AB}$ | $J_{BB'}$ |
|-----------------------|-------------------|--------------------|----------|--------------------|----------|----------|-----------|
| <b>1</b> <sup>b</sup> | AB <sub>2</sub> X | 25                 | 145      | 15                 | 143      | 38       |           |
| <b>1</b> <sup>c</sup> | ABB'X             | 26                 | 148      | 15                 | 140      |          | 370       |
|                       |                   |                    |          | 17                 | 140      |          |           |
| <b>2</b> <sup>b</sup> | A <sub>4</sub> X  | -4                 | 140      |                    |          |          |           |
| <b>3</b> <sup>d</sup> | A <sub>2</sub> X  | 24                 | 125      |                    |          |          |           |
| <b>4</b> <sup>b</sup> | A <sub>2</sub> BX | 15                 | 0        | 44                 | 157      | 18       |           |
| <b>5</b> <sup>b</sup> | AX                | 27                 | 113      |                    |          |          |           |
| <b>6</b> <sup>b</sup> | A <sub>2</sub> X  | 18                 | 137      |                    |          |          |           |
| <b>7</b> <sup>b</sup> | A <sub>2</sub> X  | 22                 | 135      |                    |          |          |           |

<sup>a</sup>  $\delta$  (ppm);  $J$  (Hz); A = B = P; X = Rh. <sup>b</sup> In C<sub>6</sub>D<sub>6</sub>. <sup>c</sup> Solid state. <sup>d</sup> In C<sub>7</sub>D<sub>8</sub>.

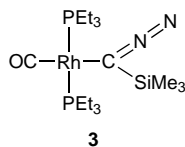
infrared spectra (pentane solution) of **1** and **2** show



intense  $\nu\text{C}(\text{N}_2)$  absorptions at 1945 and 1950  $\text{cm}^{-1}$ , respectively. These peaks are at lower frequencies than the free diazoalkane (2060  $\text{cm}^{-1}$ ). The  $^1\text{H}$  NMR spectrum of **1** shows the characteristic resonances of the phosphine ethyl substituents at 1.04, 1.16, 1.43, and 1.83 ppm, together with the sharp singlet corresponding to the SiMe<sub>3</sub> protons at 0.6 ppm (SiMe<sub>3</sub>/PEt<sub>3</sub> = 1/3). The  $^{31}\text{P}\{^1\text{H}\}$  NMR spectrum in C<sub>6</sub>D<sub>6</sub> is of the first-order AB<sub>2</sub>X type. The data are given in Table 4. In the  $^{13}\text{C}\{^1\text{H}\}$  NMR spectrum, the PEt<sub>3</sub> signals appear at 9.56 and 9.45 ppm for CH<sub>3</sub> and at 21.6 and 18.95 ppm for CH<sub>2</sub>, whereas the SiMe<sub>3</sub> carbons are found at 1.47 ppm. No signals could be detected for the carbon of the diazo group. This signal was located at 2.23 ppm in the free ligand,<sup>1b</sup> which is significantly shielded when compared to other sp<sup>2</sup> carbons. As a consequence, it may be masked by one of the phosphine carbon resonance. In agreement with this, is its presence at 11.2 ppm in **3** (*vide infra*).

For **2**, the  $^1\text{H}$  and  $^{31}\text{P}\{^1\text{H}\}$  NMR spectra both show a single broad peak for the phosphines at room temperature but the 173 K  $^{31}\text{P}\{^1\text{H}\}$  NMR spectrum in C<sub>7</sub>D<sub>8</sub> consists of a sharp doublet at -4 ppm, with  $J_{\text{RhP}} = 140$  Hz. This observation suggests that the molecule has either a fluxional structure or a static square-pyramidal structure with an apical diazo ligand.

**Preparation of Rh[C(N<sub>2</sub>)SiMe<sub>3</sub>](CO)(PEt<sub>3</sub>)<sub>2</sub> (**3**).** Two methods were developed. The approach that parallels the formation of **1**, using RhCl(CO)(PEt<sub>3</sub>)<sub>2</sub> as starting material, was not very efficient on a preparative scale (the yield was only 40%). The most convenient method was to react **1** in benzene with 1 equiv of carbon monoxide. The reaction was fast and **3** was isolated at



room temperature in 90% yield. The compound was obtained as air-sensitive yellow crystals. The two strong infrared peaks at 1961 and 1947  $\text{cm}^{-1}$  confirm the presence of the diazo group and the terminal CO ligand, respectively. The  $^{31}\text{P}\{^1\text{H}\}$  spectrum displays a doublet

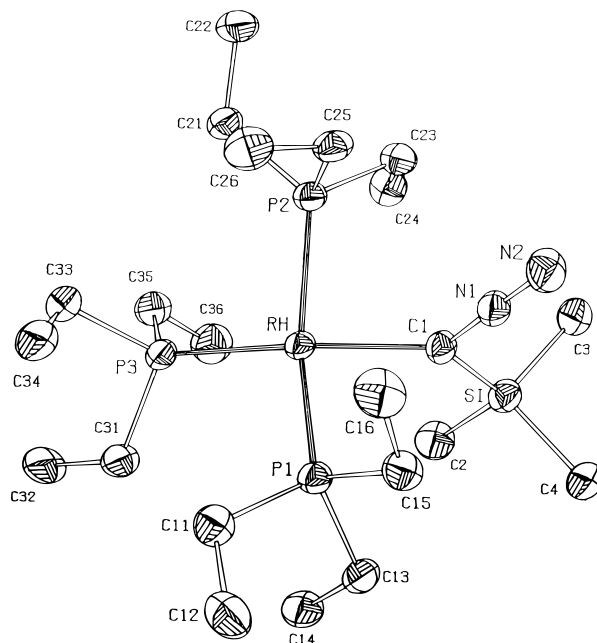


**Figure 1.** ORTEP view of the Rh[C(N<sub>2</sub>)SiMe<sub>3</sub>](PEt<sub>3</sub>)<sub>3</sub> molecule (**1**) and atomic labeling scheme. Hydrogen atoms are omitted for clarity. Ellipsoids are drawn at 50% probability.

**Table 5.** Selected Bond Distances and Angles for Rh[C(N<sub>2</sub>)SiMe<sub>3</sub>](PEt<sub>3</sub>)<sub>3</sub> (**1**)<sup>a</sup>

| Bond Distance (Å) |           |          |           |
|-------------------|-----------|----------|-----------|
| Rh-P1             | 2.310(2)  | Rh-P2    | 2.316(1)  |
| Rh-P3             | 2.259(1)  | Rh-C1    | 2.156(5)  |
| C1-Si             | 1.842(6)  | C1-N1    | 1.276(7)  |
| N1-N2             | 1.166(8)  |          |           |
| Bond Angle (deg)  |           |          |           |
| P1-Rh-P2          | 151.55(5) | P1-Rh-P3 | 101.04(5) |
| P2-Rh-P3          | 96.09(5)  | P1-Rh-C1 | 84.3(2)   |
| P2-Rh-C1          | 86.6(1)   | P3-Rh-C1 | 161.6(2)  |
| Rh-C1-Si          | 125.9(3)  | Rh-C1-N1 | 123.6(4)  |
| C1-N1-N2          | 179.7(6)  | Si-C1-N1 | 110.4(4)  |

<sup>a</sup> Values in parentheses, estimated standard deviations.

at 24 ppm ( $J_{\text{PRh}} = 125$  Hz) typical of two *trans* phosphines. The  $^1\text{H}$  NMR spectrum shows a broad resonance at 1.8 ppm for the CH<sub>2</sub> group, a quintet resonance at 1.1 ppm for the CH<sub>3</sub> group of PEt<sub>3</sub>, and a SiMe<sub>3</sub> singlet at 0.4 ppm (SiMe<sub>3</sub>/PEt<sub>3</sub> = 1/2). The  $^{13}\text{C}$  NMR spectrum displays a doublet of triplets at 11.2 ppm for the diazo carbon atom, whereas the doublet of triplets at 191.8 ppm corresponds to the terminal CO ligand. Thus, the signal of the diazo carbon is considerably shifted upfield, compared with the corresponding 40 ppm signal for PdCl[C(N<sub>2</sub>)CO<sub>2</sub>Et](PEt<sub>3</sub>)<sub>2</sub>. This result may be related to the electron-releasing character of the SiMe<sub>3</sub> substituent.

**Crystal Structure of 1.** Since few C-bonded diazoalkane complexes have been structurally characterized and no structural results are available for Rh(I) species, the crystal structure of **1** was determined. The unit cell contains the monomeric molecule shown in Figure 1. There are no unusually short intermolecular contacts. Intramolecular distances and angles are given in Table 5.

The rhodium coordination geometry can be described as square planar with a distortion due to steric crowding from PEt<sub>3</sub> (cone angle 132°). The P3-Rh-P angles (96.09(5)° and 101.04(5)°) are definitely greater than the

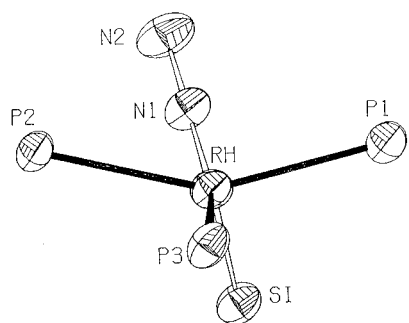


**Figure 2.** Simplified ORTEP view of the  $\text{Rh}[\text{C}(\text{N}_2)\text{SiMe}_3](\text{PEt}_3)_3$  molecule (**1**).

*cis*P–Rh–C1 angles ( $86.6(1)^\circ$  and  $84.3(2)^\circ$ ) with the less sterically demanding diazoalkane ligand. In addition to in-plane deviations from  $90^\circ$ ,  $(\text{PR}_3)_3\text{RhX}$  complexes commonly exhibit a tetrahedral distortion. With  $\text{PMe}_3$  and  $\text{PPh}_3$  (no crystallographic work available for  $\text{PEt}_3$ ), the *trans* bond angles are typically  $\sim 165^\circ$ ,<sup>24</sup> but greater distortions have been reported, for instance  $152.8^\circ$  for  $(\text{PPh}_3)_3\text{RhCl}$ .<sup>25</sup> Thus, the tetrahedral distortion found here is rather large (P1–Rh–P2 and P3–Rh–C1 angles of  $151.55(5)^\circ$  and  $161.6(2)^\circ$ , respectively). Nevertheless this cannot be regarded as a peculiarity of  $\text{PEt}_3$  since the related  $(\text{PEt}_3)_3\text{PtX}$  complexes (X = Cl, F) are much less distorted ( $\sim 175$  and  $163^\circ$ ).<sup>26</sup>

The Rh–P distances follow the pattern found in a number of tris(phosphine) complexes: the mutually *trans* Rh–P bonds are  $\sim 0.05$  Å longer than the third one, indicating that the carbene ligand does not exert a strong *trans* influence.

The (trimethylsilyl)diazomethyl group is planar and nearly orthogonal to the coordination plane. This geometry, also observed for the palladium complexes, can be ascribed to repulsive interactions between the bulky  $\text{SiMe}_3$  and  $\text{PEt}_3$  groups. The  $\text{sp}^2$  hybridization of the diazo carbon atom is apparent from the Rh–C1–N1, Rh–C1–Si, and N1–C1–Si angles ( $123.6(4)^\circ$ ,  $125.9(3)^\circ$ , and  $110.4(4)^\circ$ , respectively) and the linearity of the  $\text{CN}_2$  group ( $179.7(6)^\circ$ ). Considering the usually low precision on nitrogen atom coordinates due to the high thermal motion, the C1–N1 and N1–N2 distances are similar to those usually obtained for diazoalkanes.

If, in solution, the equivalence of the two phosphorus atoms P1 and P2 is observed (*vide supra*), indicating that the Si–C1–N1–N2 fragment lies in the C1–Rh–P3 plane, this is not the case in the solid state. In the crystal, the C1–N1–N2–Si plane makes a  $18^\circ$  angle with the P3–Rh–C1 plane (Figure 2). As a result, the P1 and P2 atoms are no longer equivalent, although their bond distances are not affected ( $2.310(2)$  and  $2.316(1)$  Å, respectively). This inequivalence is evident in the solid-state  $^{31}\text{P}\{^1\text{H}\}$  NMR spectrum, which is of  $\text{ABB}'\text{X}$  type. The complete spectrum includes central bands with a number of spinning side bands at 4 kHz, which essentially are replicas of these central bands and reveal a large  $^{31}\text{P}$  chemical shift anisotropy. The low-

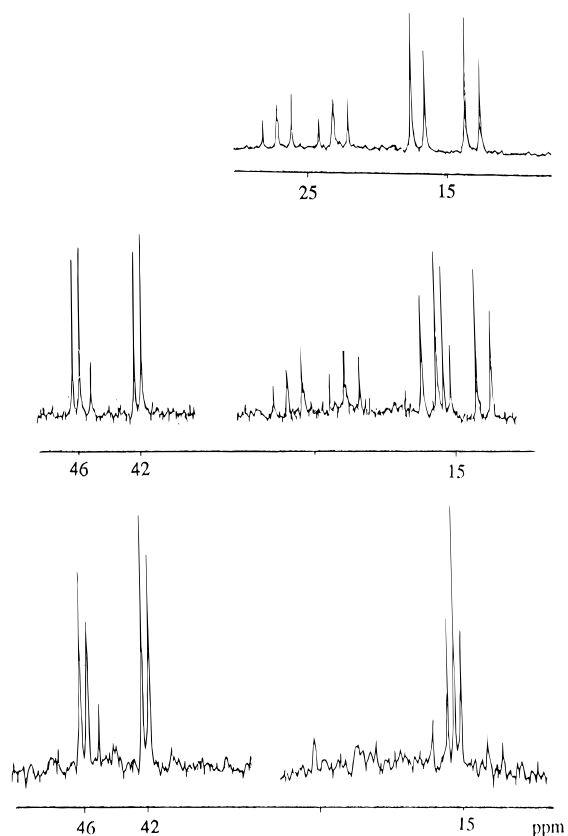
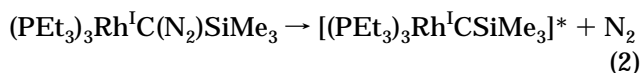


**Figure 3.** Evolution of  $^{31}\text{P}\{^1\text{H}\}$  NMR spectra of  $\text{Rh}[\text{C}(\text{N}_2)\text{SiMe}_3](\text{PEt}_3)_3$  during photolysis in  $\text{C}_6\text{D}_6$  at 330 nm.

field doublet, centered at  $\delta\text{P}_A = 26$  ppm, is attributed to the P3 atom *trans* to the diazomethyl group and bonded to rhodium with a coupling constant  $J_{\text{RhPA}} = 148$  Hz. The high-field multiplet is analyzed as part of a  $\text{BB}'\text{X}$  non-first-order spin system ( $\text{BB}'$  are the magnetically nonequivalent, mutually *trans*, P1 and P2 atoms and X is rhodium) with  $\delta\text{P}_B = 15$  ppm,  $\delta\text{P}_{B'} = 17$  ppm, the coupling constants being  $J_{\text{RhPB}} = J_{\text{RhPB}'} = 140$  Hz and  $J_{\text{PBPB}'} = 370$  Hz;  $\Delta\delta$ ,  $\nu/J = 0.66$ . The coupling of the *cis*-P atoms, normally in the range 0–50 Hz, is too small to be observed. The usual large *trans* coupling<sup>27</sup> and the absence of a resolved *cis* coupling confirms that, in the solid, the Rh–P1–P2–P3–C1 unit has a nearly square-planar geometry. These parameters agree reasonably well with those derived from the solution spectrum in  $\text{C}_6\text{D}_6$ :  $\delta\text{P}_{1,2} = 15$  ppm,  $J_{\text{RhP1,2}} = 143$  Hz,  $\delta\text{P}_3 = 25$  ppm,  $J_{\text{RhP3}} = 145$  Hz, and  $J_{\text{P1,2-P3}} = 38$  Hz. Thus, in solution, the mutually *trans*-P atoms become equivalent since crystal packing effects have been removed.

**Photolysis of 1: Synthesis of a Transient Rhodium–Carbene Species.** Photolysis of **1** is of particular interest since it behaves as precursor to an  $\alpha$ -metalated carbene (reaction 2). Room-temperature photol-



ysis of a red benzene solution ( $5 \times 10^{-2}$  M) of **1** at 330 nm has been monitored by  $^{31}\text{P}\{^1\text{H}\}$  NMR (Figure 3). The

(24) Osakada, K.; Hataya, K.; Yamamoto, T. *Inorg. Chem.* **1993**, *32*, 2360; *Organometallics* **1993**, *12*, 3358. Jones, R. A.; Real, F. M.; Wilkinson, G.; Galas, A. M. R.; Hurthouse, M. B.; Malik, K. M. A. *J. Chem. Soc., Dalton Trans.* **1980**, 511. Clegg, W.; Garner, C. D.; Heyworth, S. *Acta Crystallogr.* **1989**, *C45*, 1996. Krogsrud, S.; Komiya, S.; Ito, T.; Ibers, J. A.; Yamamoto, A. *Inorg. Chem.* **1976**, *15*, 2798.

(25) Bennett, M. J.; Donaldson, P. B. *Inorg. Chem.* **1977**, *16*, 655.

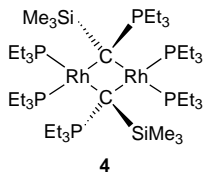
(26) Russell, D. R.; Mazid, M. A.; Tucker, P. A. *J. Chem. Soc., Dalton Trans.* **1980**, 1737.

(27) Gal, A. W.; Gosselink, J. W.; Vollenbroek, F. A. *J. Organomet. Chem.* **1977**, *142*, 357. Thewissen, D. H. M. W.; van Gaal, H. L. M. *J. Organomet. Chem.* **1979**, *172*, 69. Thewissen, D. H. M. W.; Ambrosius, H. P. M.; van Gaal, H. L. M.; Steggerda, J. J. *J. Organomet. Chem.* **1980**, *192*, 101.

spectrum at  $t = 0$  showed only the  $AB_2X$  signal due to **1**. After 30 min of irradiation, the formation of a new species **4** produced two new resonances: a doublet of doublets centered at  $\delta = 44$  ppm and a triplet at about  $\delta = 15$  ppm. After 90 min of irradiation, the reaction was complete and the formation of **4** was quantitative.

The progress of the reaction could be simultaneously monitored by the intensity loss of the infrared  $\nu(\text{CN}_2)$  absorption of **1**, which had disappeared after 90 min. Species **4** showed no IR absorption in the 1900–2200  $\text{cm}^{-1}$  range.

Complex **4** was assigned the structure  $\{\text{Rh}[\text{C}(\text{SiMe}_3)(\text{PEt}_3)](\text{PEt}_3)_2\}_2$  on the basis of NMR and IR data. It precipitated at  $-25$  °C as an oily green solid, but all attempts to isolate it at room temperature failed. The



$^1\text{H}$  NMR spectrum of **4** exhibits two quartets in 2/1 ratio at 1.38 and 1.67 ppm, corresponding to the  $\text{CH}_2$  groups of the triethylphosphines bonded to Rh and to the phosphorus ylide, respectively.  $\text{SiMe}_3$  is characterized by a singlet at  $\delta = 0.66$  ppm.  $^{31}\text{P}\{^1\text{H}\}$  spectra recorded at 36.43 and 101.22 MHz had no effect on the signal positions, thereby confirming that the  $^{31}\text{P}$  splittings are due to coupling and not to multiple species. This also is confirmed by the COSY  $^{31}\text{P}-^{31}\text{P}\{^1\text{H}\}$  NMR experiment, which shows a doublet of doublet and a pseudo-triplet. The doublet of doublets at 44 ppm results from the two equivalent  $\text{PEt}_3$  ligands bonded to rhodium ( $J_{\text{PRh}} = 157$  Hz) and coupled to the ylide phosphorus atom ( $J_{\text{PP}} = 18$  Hz). The pseudo triplet at  $\delta = 15$  ppm shows no coupling with rhodium. This signal is in the range usually observed for phosphorus ylides.<sup>28</sup> Interestingly, the presence of  $\text{SiMe}_3$  and  $\text{Rh}(\text{PEt}_3)_2$  as  $\text{R}_1$  and  $\text{R}_2$  substituents on the phosphorus ylide  $\text{CR}_1\text{R}_2=\text{PEt}_3$  only has a small effect on its  $^{31}\text{P}$  chemical shift, which indicates that the electronic effects of these two groups may be equal and opposite. The  $^2J_{\text{RhP}}$  coupling constant of the ylide phosphorus atom with rhodium is nearly 0, in agreement with the low value already reported for the phosphorus ylide bridging two rhodium centers in  $[\text{Rh}(\text{CO})_2(\text{CH}_2)\text{PMe}_2(\text{CH}_2)]_2$ . A higher  $^2J_{\text{RhP}}$  value of 24.9 Hz has been reported in the case of a phosphorus ylide chelating a single rhodium center.<sup>29</sup> In dilute solutions, the photolysis proceeded similarly, as indicated by electronic spectroscopy. The yellow solution (25 °C) exhibited absorption bands at 340 and 290 nm (Figure 4), in the range expected for square-planar rhodium(I) complexes.<sup>30</sup> As the photolysis progressed, no significant color change was apparent in the solution, but a new band developed at 585 nm. The isosbestic points at 310 and 435 nm are consistent with the

(28) In free  $\text{Et}_3\text{P}=\text{CH}_2$ , the  $^{31}\text{P}$  NMR chemical shift is  $\delta = 16.9$  ppm ( $J_{\text{PC}} = 113.2$  Hz). For free  $\text{Et}_3\text{P}=\text{CHSiMe}_3$ , the value is not significantly different: Grim, S. O. In *Phosphorus 31 NMR Spectroscopy in Stereochemical Analysis, Organic Compounds and Metal Complexes*; Verkade, J. G., Quin, L. D., Eds.; VCH: Deerfield Beach, FL, 1987; p 645.

(29) Lapinski, R. L.; Hue, H.; Grey, R. A. *J. Organometal. Chem.* **1979**, *174*, 213.

(30) Brady, R.; Flynn, B. R.; Geoffroy, G. L.; Gray, H. B.; Peone, J., Jr.; Vaska, L. *Inorg. Chem.* **1976**, *15*, 1485.

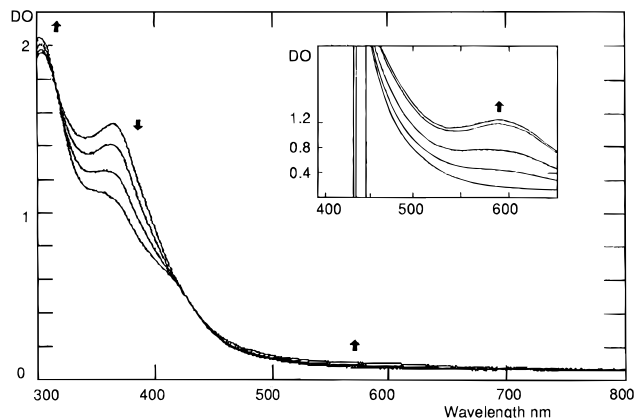
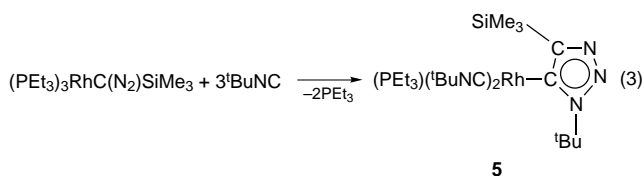


**Figure 4.** UV spectra during irradiation of  $\text{Rh}[\text{C}(\text{N}_2)\text{SiMe}_3](\text{PEt}_3)_3$  (**1**) in  $\text{C}_6\text{H}_6$ ,  $c = 5 \times 10^{-2}$  M.

presence of only two species, which have been identified by  $^{31}\text{P}$  NMR spectroscopy as the starting compound **1** and the ylide dimer **4**.

**Reaction of 1 with Isocyanides: [3 + 2] Dipolar Cycloaddition.** The reaction of **1** with excess of  $^t\text{BuNC}$  (ratio 1/4) at room temperature ( $\text{C}_6\text{H}_6$ ) afforded the triazole complex **5** in high yield (reaction 3). Air-



sensitive yellow crystals of *trans*-[1-*tert*-butyl-4-(trimethylsilyl)-1,2,3-triazolato]triethylphosphinebis(*tert*-butyl isocyanide)rhodium(I) (**5**) were obtained by slow crystallization from cyclopentane. When  $^n\text{BuNC}$  was used, only one  $\text{PEt}_3$  ligand was substituted and  $\text{Rh}[\text{C}(\text{SiMe}_3)\text{N}_2\text{N}(^n\text{Bu})](^n\text{BuNC})(\text{PEt}_3)_2$  (**6**) was precipitated as yellow crystals. In the infrared spectrum, the complexes display single  $\nu(\text{C}\equiv\text{NR})$  absorptions at 2100  $\text{cm}^{-1}$  for **5** (Nujol mull) and at 2113  $\text{cm}^{-1}$  for **6** (in  $\text{C}_6\text{H}_6$ ), typical of terminal isocyanides.<sup>31</sup> As evidenced from  $^1\text{H}$ ,  $^{31}\text{P}$ , and  $^{13}\text{C}$  NMR spectroscopies, only one phosphine ligand with two magnetically inequivalent isocyanide groups is present in **5**, whereas two *trans*  $\text{PEt}_3$  and one  $^n\text{BuNC}$  ligand are found in **6**. In order to characterize **5** unambiguously and because there are no precedents for C-bonded 1*H*-1,2,3-triazolato complexes, a single-crystal X-ray analysis of **5** was undertaken.

**Crystal Structure of 5.** The ORTEP drawing for the complex is given in Figure 5, along with the atomic numbering scheme. Bond distances and angles are listed in Table 6. The unit cell of **5** contains monomeric molecules. The geometry around Rh corresponds to a distorted square plane, with rhodium coordinated to two *trans tert*-butyl isocyanides, one triethylphosphine, and the carbon atom of the 1*H*-1,2,3-triazolato ligand. The relatively bulky  $\text{PEt}_3$  ligand makes the adjacent angles  $\text{P}-\text{Rh}-\text{C31} = 94.4(2)^\circ$ ,  $\text{P}-\text{Rh}-\text{C41} = 93.7(2)^\circ$  greater than those on the side of the less sterically demanding triazolato ligand ( $\text{C1}-\text{Rh}-\text{C31} = 88.7(3)^\circ$ ,  $\text{C1}-\text{Rh}-\text{C41} = 83.2(3)^\circ$ ). The *trans* angles are  $\text{C31}-\text{Rh}-\text{C41} = 171.9(3)^\circ$  and  $\text{P}-\text{Rh}-\text{C1} = 176.8(2)^\circ$ . The  $\text{Rh}-\text{C}$  and

(31) Nakamoto, K. *Infrared and Raman Spectra of Inorganic and Coordination Compounds*, 4th ed.; J. Wiley & Sons: New York, 1986.

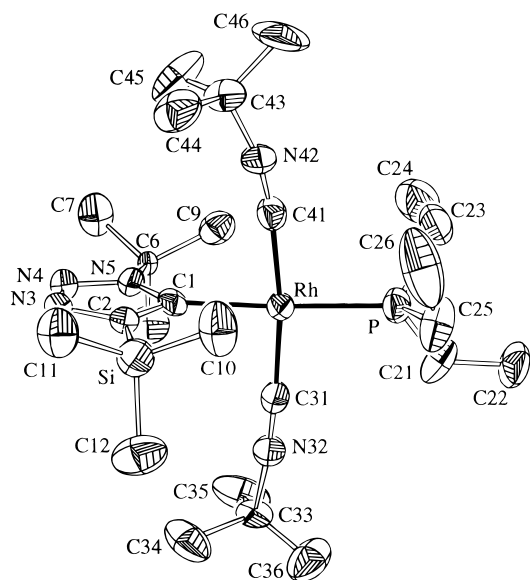


**Figure 5.** Simplified ORTEP view of  $\text{Rh}[\text{CC}(\text{SiMe}_3)\text{-N}_2\text{N}(\text{tBu})](\text{tBuNC})_2(\text{PET}_3)$  (**5**), and atomic labeling scheme. Hydrogen atoms are omitted for clarity. Only one set of positions is represented for the disordered atoms in the  $\text{PET}_3$  and  $\text{tBuNC}$  ligands. Ellipsoids are drawn at 50% probability.

**Table 6. Selected Interatomic Distances and Bond Angles for**

**$\text{Rh}[\text{CC}(\text{SiMe}_3)\text{N}_2\text{N}(\text{tBu})](\text{tBuNC})_2(\text{PET}_3)$  (**5**)**

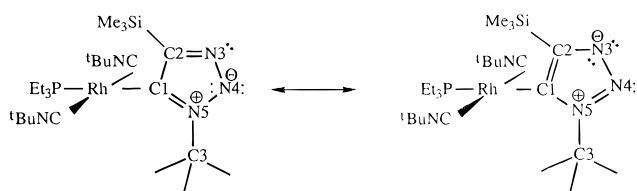
| Bond Distance (Å)     |           |                            |           |
|-----------------------|-----------|----------------------------|-----------|
| Rh–P                  | 2.265(2)  | Rh–C1                      | 2.080(7)  |
| Rh–C31                | 1.953(8)  | Rh–C41                     | 1.960(8)  |
| C1–C2                 | 1.430(10) | N3–C2                      | 1.385(10) |
| N3–N4                 | 1.301(10) | N4–N5                      | 1.370(10) |
| N5–C1                 | 1.380(9)  | N5–C6                      | 1.496(9)  |
| N32–C31               | 1.142(11) | N42–C41                    | 1.146(10) |
| N32–C33 <sup>a</sup>  | 1.56(2)   | N42–C43 <sup>a</sup>       | 1.40(2)   |
| N32–C33' <sup>a</sup> | 1.35(4)   | N42–C43'' <sup>a</sup>     | 1.57(4)   |
| Bond Angle (deg)      |           |                            |           |
| P–Rh–C1               | 176.8(2)  | C1–Rh–C31                  | 88.7(3)   |
| P–Rh–C31              | 94.4(2)   | C1–Rh–C41                  | 83.2(3)   |
| P–Rh–C41              | 93.7(2)   | C31–Rh–C41                 | 171.9(3)  |
| Rh–P–C21              | 116.8(7)  | Rh–C1–C2                   | 127.2(5)  |
| Rh–C1–N5              | 130.3(5)  | Si–C2–C1                   | 131.4(6)  |
| Si–C2–N3              | 120.7(6)  | N3–N4–N5                   | 107.6(6)  |
| C2–N3–N4              | 110.2(7)  | N4–N5–C1                   | 111.8(6)  |
| N4–N5–C6              | 117.4(5)  | C1–N5–C6                   | 130.6(6)  |
| N5–C1–C2              | 102.5(6)  | N3–C2–C1                   | 107.9(6)  |
| Rh–C41–C42            | 172.6(7)  | C41–N42–C43                | 164.9(13) |
| Rh–C31–N32            | 177.2(7)  | C41–N42–C43'' <sup>a</sup> | 153.9(19) |
| C31–N32–C33           | 167.9(10) | C31–N32–C33' <sup>a</sup>  | 169.7(14) |

<sup>a</sup> Bonds and angles involving disordered atoms.

Rh–P distances are similar to those reported for other  $\text{Rh}(\text{I})\text{-CNR}^{32}$  and  $\text{Rh}(\text{I})\text{-PR}_3^{24}$  bonds.

The C1–C2–N3–N4–N5 heterocycle is planar and nearly perpendicular to the least-squares plane through P1, C31, C41, Rh, and C1, the dihedral angle being  $87.5(3)^\circ$ . The two terminal isocyanides are roughly linear and slightly bent toward the heterocycle. This ground-state geometry is presumably favored by the steric requirements of the ligands. The  $\text{sp}^2$  hybridization of the N5 atom is indicated by the C1–N5–N4, C1–N5–C6, and N4–N5–C6 angles ( $111.8(6)^\circ$ ,  $130.6(6)^\circ$ , and  $117.4(5)^\circ$ , respectively) and the planarity of the heterocycle.<sup>33</sup> Thus, the triazole ring is aromatic and can be described by the two limiting resonance struc-

**Scheme 1**



tures depicted in Scheme 1. This agrees with the downfield shifts of the methyl resonances in the N5-bonded  $\text{tBu}$  group, which are observed at 2.28 ppm in  $^1\text{H}$  NMR and 32.89 ppm in  $^{13}\text{C}\{^1\text{H}\}$  NMR spectra. The corresponding values are 0.96 ( $^1\text{H}$ ) and 30.08 ppm ( $^{13}\text{C}$ ) for the  $\text{tBu}$  groups of the terminal isocyanides.

In order to get more insight into these reactions, we studied the reaction of **1** with increasing amounts of  $\text{tBuNC}$  in  $\text{C}_6\text{H}_6$  at  $20^\circ\text{C}$  ( $x = \text{tBuNC}/\mathbf{1}$  molar ratio). The reactions were followed by  $^{31}\text{P}$  NMR and IR spectroscopies. No signal broadening was observed in  $^{31}\text{P}$  NMR, and individual resonances were clearly visible for the different species at room temperature.

For  $x < 1$ , the spectrum showed resonances for three compounds: the  $\text{AB}_2\text{X}$  system of **1**, a doublet at  $\delta = 22$  ppm ( $J_{\text{Rh-P}} = 135$  Hz) corresponding to the two equivalent phosphines of  $\text{Rh}[\text{C}(\text{N})_2\text{SiMe}_3](\text{PET}_3)_2(\text{tBuNC})$  (**7**), and free  $\text{PET}_3$  at  $\delta = -18$  ppm. The IR spectrum consisted of strong absorptions due to the terminal isocyanide ( $2050\text{ cm}^{-1}$ ), the C-bonded diazo ligand ( $1955\text{ cm}^{-1}$ ) of **7**, and the diazo group ( $1945\text{ cm}^{-1}$ ) of **1**.

As  $x$  was increased from 1 to  $\sim 2.2$ , **7** slowly disappeared and four new species appeared. The proportions were dependent on  $x$ . None of these species was isolated. In all cases, a doublet at  $\delta = 20$  ppm ( $J_{\text{Rh-P}} = 137$  Hz) was observed as the major species. The IR spectrum of the solution showed several strong absorptions near  $2100\text{--}2050$  and  $1950\text{--}1925\text{ cm}^{-1}$ , indicating the presence of both terminal isocyanides and C-bonded diazo ligands.

Increasing  $x$  to 3 or 5 resulted in a higher yield of **5**, which became the major product, whereas an unidentified minor species became apparent at  $\delta = 22$  ppm ( $J_{\text{Rh-P}} = 105$  Hz). The strong vibrations of terminal isocyanides were still present at  $2100\text{--}1980\text{ cm}^{-1}$ , but new absorptions characteristic of a  $\text{C}=\text{N}$  double bond grew at  $1616\text{--}1550\text{ cm}^{-1}$ , suggesting the presence of bridging isocyanide.<sup>34</sup>

**Discussion**

Organic diazoalkanes are well-known to generate carbenes (thermally or photochemically) and/or to give rise to  $[3 + 3]$  or  $[3 + 2]$  cycloaddition reactions. This work shows that the rhodium-substituted triethylsilyldiazomethyl complex, **1**, behaves similarly.

When photolyzed at 330 nm, **1** produces a transient electrophilic carbene, **A**, which is trapped by  $\text{PET}_3$  to give

(32) Mann, K. R.; Lewis, N. S.; Gray, H. B.; Gordon, J. B., II. *Inorg. Chem.* **1978**, *17*, 828. Jones, W. D.; Duttweiler, R. P., Jr.; Feher, F. J. *Inorg. Chem.* **1990**, *29*, 1505. Jones, W. D.; Hessel, E. T. *Organometallics* **1990**, *9*, 718.

(33) Barton, D.; Allis, W. D. In *Comprehensive Organic Chemistry*; Sammer, P. G., Ed.; The City University: London, 1979; Vol. IV, Chapter 7, p 361. Parkanyl, L.; Kalman, A.; Argay, G.; Schawartz, J. *Acta Crystallogr.* **1977**, *B33*, 3102. Nagawa, Y.; Goto, M.; Honda, K.; Nakanishi, H. *Acta Crystallogr.* **1987**, *C43*, 147.

(34) Belt, S. T.; Duckett, S. B.; Haddleton, D. M.; Perutz, R. N. *Organometallics* **1989**, *8*, 748. Gill, D. S.; Barker, P. K.; Green, M.; Paddick, K. E.; Murray, M.; Welch, A. J. *J. Chem. Soc., Chem. Commun.* **1981**, 986.



Scheme 2

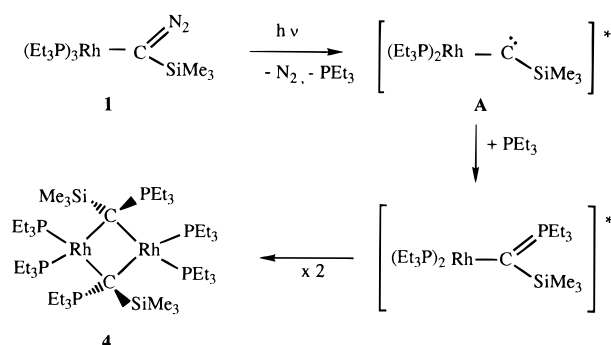


Chart 1

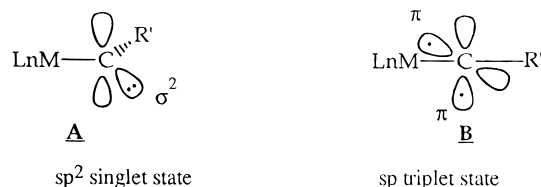
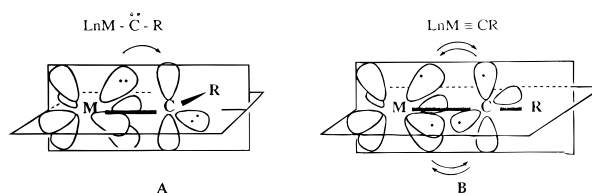


Chart 2



Scheme 3

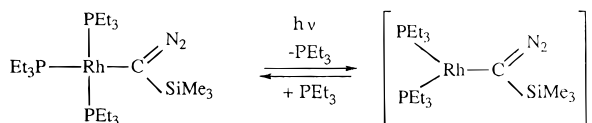
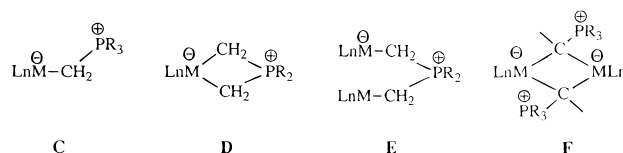


Chart 3



the binuclear ylide complex **4**. A possible pathway for the generation of **4** is shown in Scheme 2.

The first step is the formation of the 2-coordinated carbon atom  $RR'C:$ , R, and R' being the metallic  $L_nM$  fragment,  $(PEt_3)_3Rh$ , and the  $SiMe_3$  group, respectively. This species may be viewed as a transition metal-substituted carbene. The electronic structure of the ground state of organic carbenes  $RR'C:$  has been extensively studied. Two states are energetically accessible: a triplet ground state and a singlet excited state that lies a few kilocalories per mole higher in energy (Chart 1). Examples of carbenes in both states have been reported, and by extension, the name of carbene has been retained for the divalent carbon in the singlet state and methylene or alkylidene for the triplet state. Moreover, it is now well established that electronegative substituents stabilize the singlet ground state **A**, while electropositive ones stabilize the triplet state **B**. Recently, the synthesis of stable divalent carbon atoms substituted by heteroatoms was reported. Stable methylenes species have been obtained with phosphorus donor substituents<sup>35</sup> while sterically hindered N ligands produced singlet carbene.<sup>36</sup> In the field of organometallic chemistry, extensive work has been done on the synthesis, structural characterization, and reactivity of carbenes and alkylidenes bonded to transition metal fragments. Electrophilic Fischer carbenes and nucleophilic Schrock alkylidenes illustrate the influence of the metal electronic structure on the reactivities of these species.<sup>37</sup>

The transient rhodium-substituted carbene synthesized in this work behaves as an electrophile; *i.e.*, it has a singlet ground state, **A**. Stabilization of this singlet state results from the presence of the low-spin, electron-

rich, 15e  $(PEt_3)_3Rh$  fragment that possesses a  $d_{xy}$  lone pair ( $d_{xy}$ ) that is able to donate electron density into the empty  $p\pi$  orbital of the carbon atom (Chart 2).

The singlet carbene **A** could be considered as an isomeric form of the metal carbyne compound **B**. Such a compound would result from the reaction of the triplet alkylidyne species  $:CR$  with a high spin or electron poor metal fragment. This is not possible for electron-rich late transition metal fragments due to the absence of suitable unfilled orbitals. Consequently, the electronic properties of the  $d^8$  Rh fragments favor the stabilization of **A**, so that **1** acts as a precursor of singlet carbene.

Formation of an ylide intermediate is expected since photolysis at 330 nm activates not only the  $CN_2$  fragment<sup>38</sup> but also the rhodium–phosphine bonds.<sup>39</sup> The observation that photolysis takes more time when it is conducted in the presence of excess phosphine indicates that the reaction indeed proceeds *via* photoinduced labilization of a phosphine ligand to form the coordinatively unsaturated 14e complex  $(PEt_3)_2RhC(N_2)SiMe_3$  and free  $PEt_3$  (Scheme 3). Such a reaction has been shown previously to be the crucial step in photoactivation of alkanes by rhodium complexes.<sup>40</sup> No evidence for the existence of the monomeric metal-substituted ylide complex  $[(PEt_3)_3Rh](SiMe_3)C=PEt_3$  was observed even with excess of  $PEt_3$ . This is not surprising considering that monomeric ylides of late transition metals are unknown.<sup>41</sup> Most of the reported phosphorus ylides are bound to transition metals as monodentate (**C**), chelating (**D**), or bridging (**E**, **F**) ligands (Chart 3). All known rhodium ylides belong to categories **D** and **E**, and **5** is the first rhodium compound of class **F**.

(38) Chapman, O. L.; Chang, C. C.; Kolc, J.; Jung, M. E.; Lowe, J. A.; Barton, T. J.; Tumej, M. L. *J. Am. Chem. Soc.* **1976**, *98*, 7844. Chedel, M. R.; Skoglund, M.; Kreeger, R. L.; Shechter, H. *J. Am. Chem. Soc.* **1976**, *98*, 7846.

(39) Geoffroy, G. L.; Denton, D. A.; Keeney, M. E.; Bicks, R. R. *Inorg. Chem.* **1976**, *15*, 2382.

(40) Sakakura, T.; Tanaka, M. *J. Chem. Soc., Chem. Commun.* **1987**, 758. Wink, D. A.; Ford, P. C. *J. Am. Chem. Soc.* **1987**, *109*, 436. Spillet, C. T.; Ford, P. C. *J. Am. Chem. Soc.* **1989**, *111*, 1932.

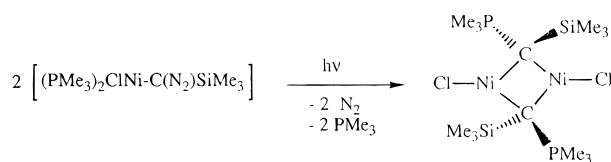
(41) Weber, L. In *The Chemistry of Metal Carbon Bond*; Hartley, F. R.; Patai, S., Eds.; John Wiley & Sons: New York, 1982; Chapter 3, p 93. Kaska, W. C. *Coord. Chem. Rev.* **1983**, *48*, 1. Schmidbaur, H.; Angew. Chem., Int. Ed. Engl. **1983**, *22*, 907. Schmidbaur, H.; Pichl, R.; Muller, G. *Angew. Chem., Int. Ed. Engl.* **1986**, *25*, 574.

(35) Igau, A.; Baccaredo, A.; Trinquier, G.; Bertrand, G. *Angew. Chem., Int. Ed. Engl.* **1989**, *28*, 621. Dixon, D. A.; Dobbs, K. D.; Arduengo, A. J.; Bertrand, G. *J. Am. Chem. Soc.* **1991**, *113*, 8782.

(36) Arduengo, A. J.; Harlow, R. L.; Klene, M. *J. Am. Chem. Soc.* **1991**, *113*, 361.

(37) Dötzt, K. H.; Fischer, H.; Hofmann, P.; Kreissl, F. R.; Schubert, U.; Weiss, K. *Transition Metal Carbenes Complexes*; Verlag Chemie: Deerfield Beach, FL, 1984. Kostic, N. M.; Fenske, R. F. *Organometallics* **1982**, *1*, 974; *J. Am. Chem. Soc.* **1981**, *103*, 4677. Carter, E. A.; Goddard, W. A., III *J. Am. Chem. Soc.* **1986**, *108*, 4746, 2180, and references therein.

## Scheme 4



Nevertheless, a few compounds with phosphorus ylides bridging two transition metals have been obtained by reacting a phosphine with electrophilic  $L_nM\equiv CR$  complexes:  $(CO)_4Re(\mu CO)(\mu CPh(PMe_3))W(CO)_4$ <sup>42</sup> and  $[Cp(CO)Mn\{\mu-C(4-MeC_6H_4)(PR_3)\}\{\mu-CO\}Pt(PR_3)_2]-[BF_4]$ .<sup>43</sup> The only other complex with two ylide bridges is one that was isolated in our laboratory from the photolysis product of the related nickel(II) diazo complex (Scheme 4).<sup>8</sup>

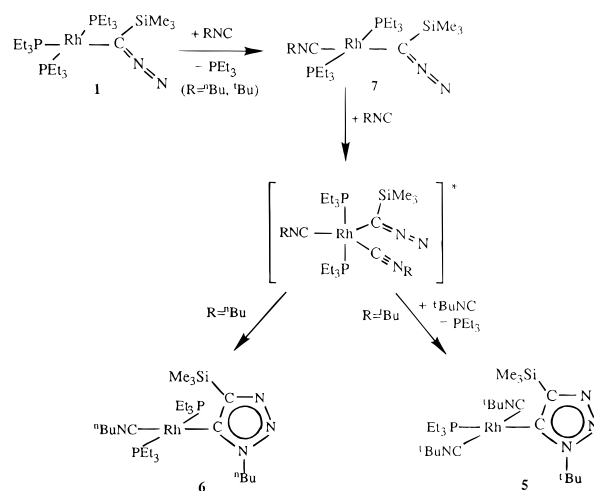
In contrast to the above, the reaction of  $(PEt_3)_3Rh[C(N_2)SiMe_3]$  with isocyanide proceeds through a different pathway. Isocyanides stabilize metal centers over a large range of oxidation states. In the last 20 years, these ligands have received special attention due to their electronic similarity to carbon monoxide. They are good  $\sigma$ -donor and  $\pi$ -acceptor ligands, can coordinate through  $\eta^1$  and  $\eta^2$  modes, and give rise to migratory insertion reactions into transition metal–carbon bond.<sup>44</sup> However, their capability to act as 1,2-dipoles and to give [2 + 2] or [2 + 3] cycloaddition reactions is not well documented.<sup>45</sup>

Few reactions of organic diazoalkanes with isocyanides have been described, and in most cases, they proceed via  $N_2$  evolution to give keteneiminyll species. To our knowledge, only one example of 1*H*-1,2,3-triazole has been reported. It was obtained as a byproduct (20% yield) from the reaction of diazoalkane with isocyanide, catalyzed by a copper complex.<sup>46</sup>

The few known metal complexes containing  $\sigma$ -bonded keteneiminyll ligands result from the reaction of isocyanides with manganese and rhenium carbene complexes<sup>47</sup> or from insertion of a diazoalkane unit into a cobalt–isocyanide bond.<sup>48</sup> We did not observe analogous reactions when  $^nBuNC$  and  $^tBuNC$  were reacted with **1**, with or without photolysis.

Scheme 5 is a summary of the species that were characterized during the reaction of isocyanides with **1**. The proposed mechanism for formation of the various products can be described as a succession of addition–

## Scheme 5



elimination reactions, with five coordinate species as intermediates. These are well-documented reaction pathways for  $d^8$  square-planar complexes. The first step involves the substitution of the phosphine *trans* to the diazoalkyl group by the isocyanide, a better  $\sigma$ -donor ligand. Addition of a second RNC molecule is followed by insertion into the Rh–diazo carbon bond. This leads to the formation of the 1*H*-1,2,3-triazole C bonded to rhodium, *via* a fast cycloaddition. The reaction stops there for  $R = ^nBu$  and **6** is isolated. With *tert*-butyl isocyanide, substitution of a second phosphine remains possible. Moreover, getting **5** from **7** suggests an isomerization reaction through a five-coordinate intermediate. The three competitive reactions—substitution, isomerization, and insertion—could explain the large number of species observed when  $x = 2$ . An excess of  $^tBuNC$  could produce a second migratory insertion of isocyanide into the rhodium–carbon bond of **5**, in agreement with the presence of the C=N vibrations for  $\eta^1$ -bonded isocyanides in the infrared spectrum.

**Acknowledgment.** M.J.M thanks the Ministère des Affaires Étrangères, the Ministère de l'Éducation du Québec (Projet Intégré France–Québec), and the Université de Montréal (Canada) for financial support (postdoctoral fellowship). This work was made possible by travel grants in the framework of the NATO Research Program for International Cooperation between M.D. and H.B.G. (890109). Material support through the Centre National de la Recherche Scientifique, the Université P. Sabatier, and the Natural Sciences and Engineering Research Council of Canada is also gratefully acknowledged. Research at Caltech was supported by the National Science Foundation. Contribution 8773 from the Division of Chemistry and Chemical Engineering, California Institute of Technology.

**Supporting Information Available:** Temperature factors, parameters of the hydrogen atoms, and bond distances and angles for **1** and **5**, <sup>31</sup>P NMR spectra and COSY <sup>31</sup>P–<sup>31</sup>P NMR spectrum of **1** and geometry of the disordered phosphine and isocyanide ligands for **5** (14 pages). Ordering information is given on any current masthead page.

OM950490H

(42) Kreissl, F. R.; Friedrich, P.; Lindner, T. L.; Huttner, G. *Angew. Chem., Int. Ed. Engl.* **1977**, *16*, 314. Vedelhoven, W.; Neugebauer, D.; Kreissl, F. R. *J. Organomet. Chem.* **1981**, *217*, 183.

(43) Jeffery, J. C.; Navarro, R.; Razay, H.; Stone, F. G. A. *J. Chem. Soc., Dalton Trans.* **1981**, 2471.

(44) Yamamoto, Y.; Yamazaki, H. *Inorg. Chem.* **1974**, *13*, 438. Gill, D. S.; Barker, P. K.; Green, M.; Paddick, K. E.; Murray, M.; Welch, A. *J. Chem. Soc., Chem. Commun.* **1981**, 986. Durfee, L. D.; Rothwell, I. P. *Chem. Rev.* **1988**, *88*, 1059. Carmona, E.; Palma, P.; Paneque, M.; Poveda, M. L. *Organometallics* **1990**, *9*, 583.

(45) Huisgen, R. *Angew. Chem., Int. Ed. Engl.* **1963**, *2*, 565.

(46) Muramatsu, M.; Obata, N.; Takizawa, T. *Tetrahedron Lett.* **1973**, *23*, 2136.

(47) Fischer, E. O.; Schambeck, W.; Kreissl, F. R. *J. Organomet. Chem.* **1979**, *169*, C27. Fischer, E. O.; Schambeck, W. *J. Organomet. Chem.* **1980**, *201*, 311. Aumann, R. *Angew. Chem., Int. Ed. Engl.* **1988**, *27*, 1456.

(48) Strecker, B.; Werner, H. *Angew. Chem., Int. Ed. Engl.* **1990**, *29*, 275.